

Geophysical Research Letters

Supporting Information for

Volcanic Climate Warming through Radiative and Dynamical Feedbacks of SO₂ Emissions

Scott D. Guzewich^{1,6*}, Luke D. Oman^{1,6}, Jacob A. Richardson^{2,1,5,6}, Patrick L. Whelley^{2,1,5,6},
Sandra T. Bastelberger^{2,1,5,6}, Kelsey E. Young¹, Jacob E. Bleacher^{3,1}, Thomas J. Fauchez^{4,1,6},
Ravi K. Kopparapu^{1,6}

¹NASA Goddard Space Flight Center; Greenbelt, MD, USA.

²University of Maryland, College Park, MD, USA.

³NASA Headquarters, Washington, DC, USA.

⁴Universities Space Research Association, Columbia, MD, USA.

⁵Center for Research and Exploration in Space Science and Technology, NASA/GSFC,
Greenbelt, MD, USA 20771

⁶NASA GSFC Sellers Exoplanet Environments Collaboration, Greenbelt, MD, USA 20771

Contents of this file

Figures S1 to S7

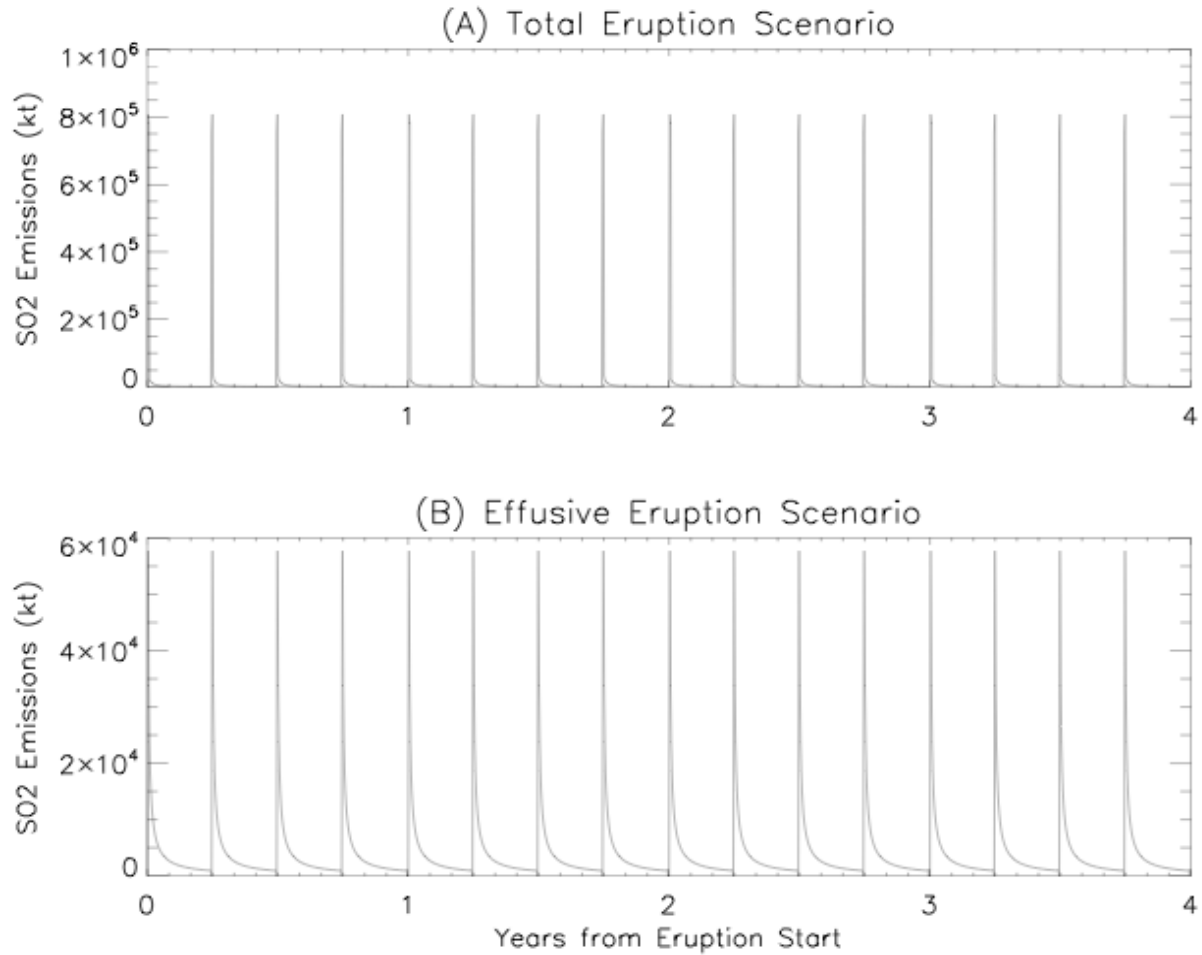


Fig. S1. Emitted SO₂ over the four year long eruption. (A) Total emitted mass of SO₂ over the four years of the simulated eruption in kilotons and (B) total effusively emitted mass of SO₂. 20% of the total mass is emitted effusively into the surface-3 km altitude atmospheric layer and

80% is emitted in four explosive eruptions per year into the upper troposphere and lower stratosphere.

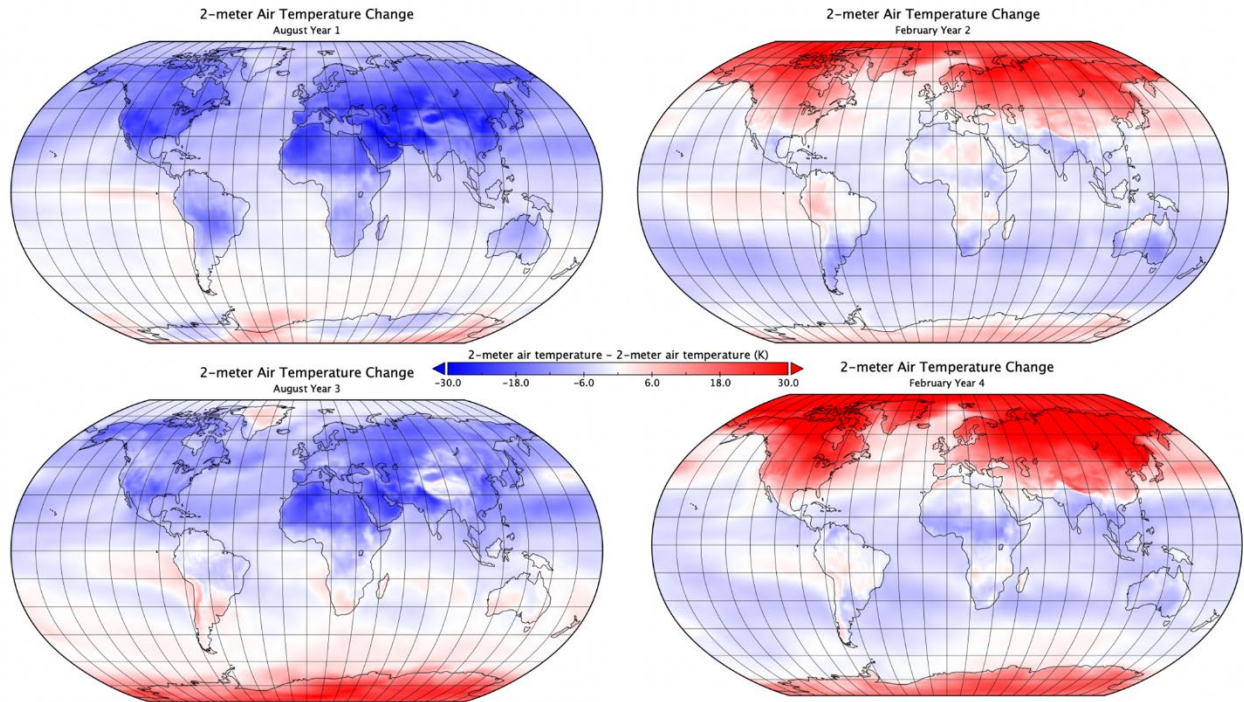


Fig. S2. Summer cooling and winter warming following the eruption. Change (eruption-baseline) in monthly mean 2 m air temperature (K) for August in simulation Year 1 (upper left), February in Year 2 (upper right), August Year 3 (lower left), and February Year 4 (lower right).

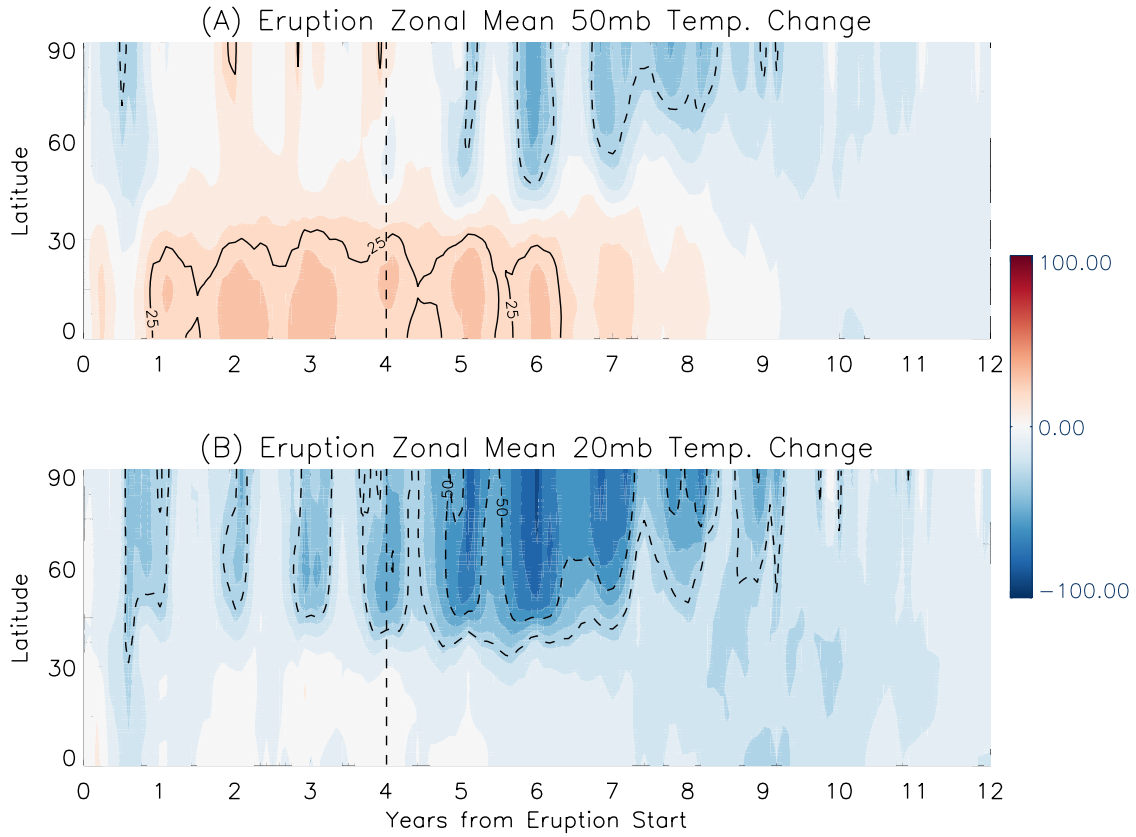


Fig. S3. The stratospheric arctic oscillation is strongly positive due to a stronger meridional temperature gradient. (A) Zonal mean temperature change (K) of the eruption simulation relative to the baseline simulation as a function of time at 50 mb and at (B) 20 mb.

the -25 K and -50 K contours with dashed lines. The vertical dashed line represents the end of the eruption.

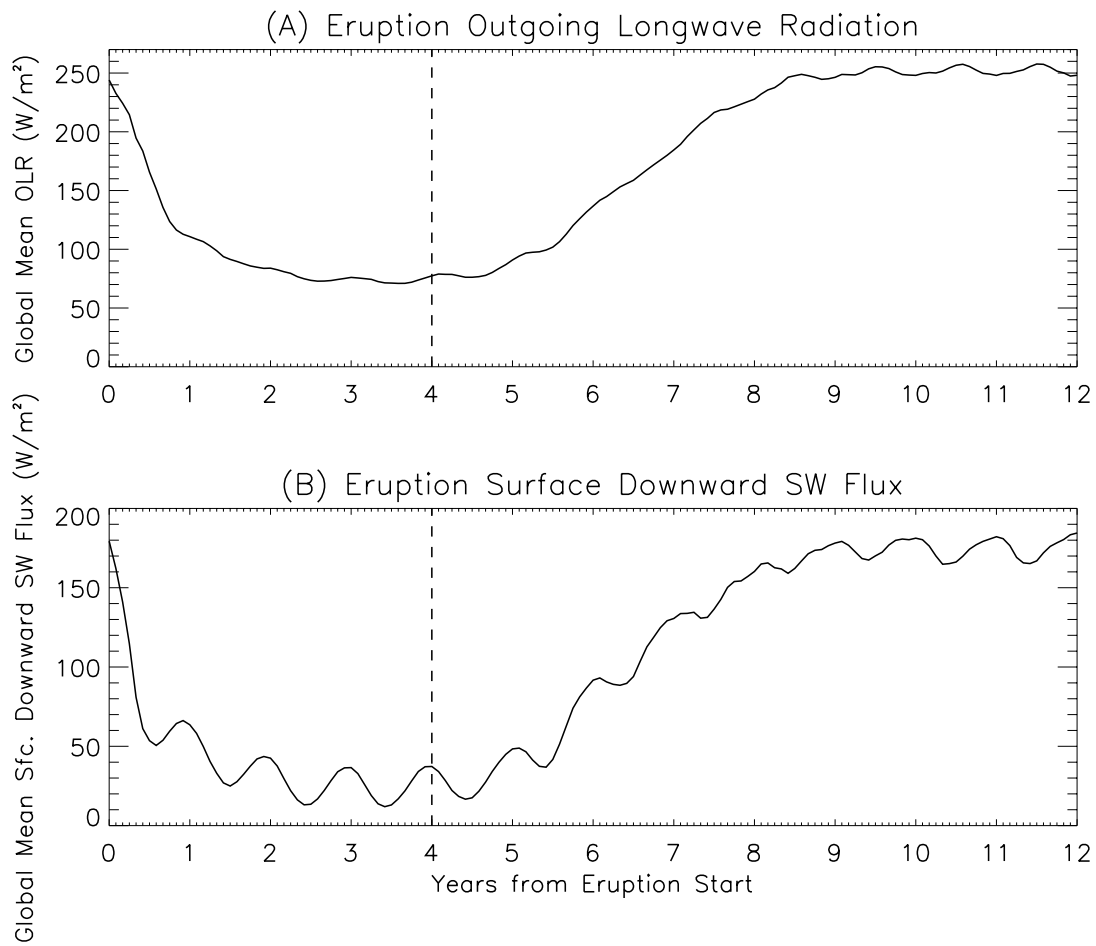


Fig. S4. Global change in longwave and shortwave radiation due to the eruption. (A) Zonal average change in outgoing longwave radiation (W/m^2) relative to the baseline simulation as function of time and (B) global area-weighted outgoing longwave radiation

function of time and (B) global area-weighted outgoing longwave radiation (W/m^2) in the eruption simulation. The vertical dashed line represents the end of the eruption.

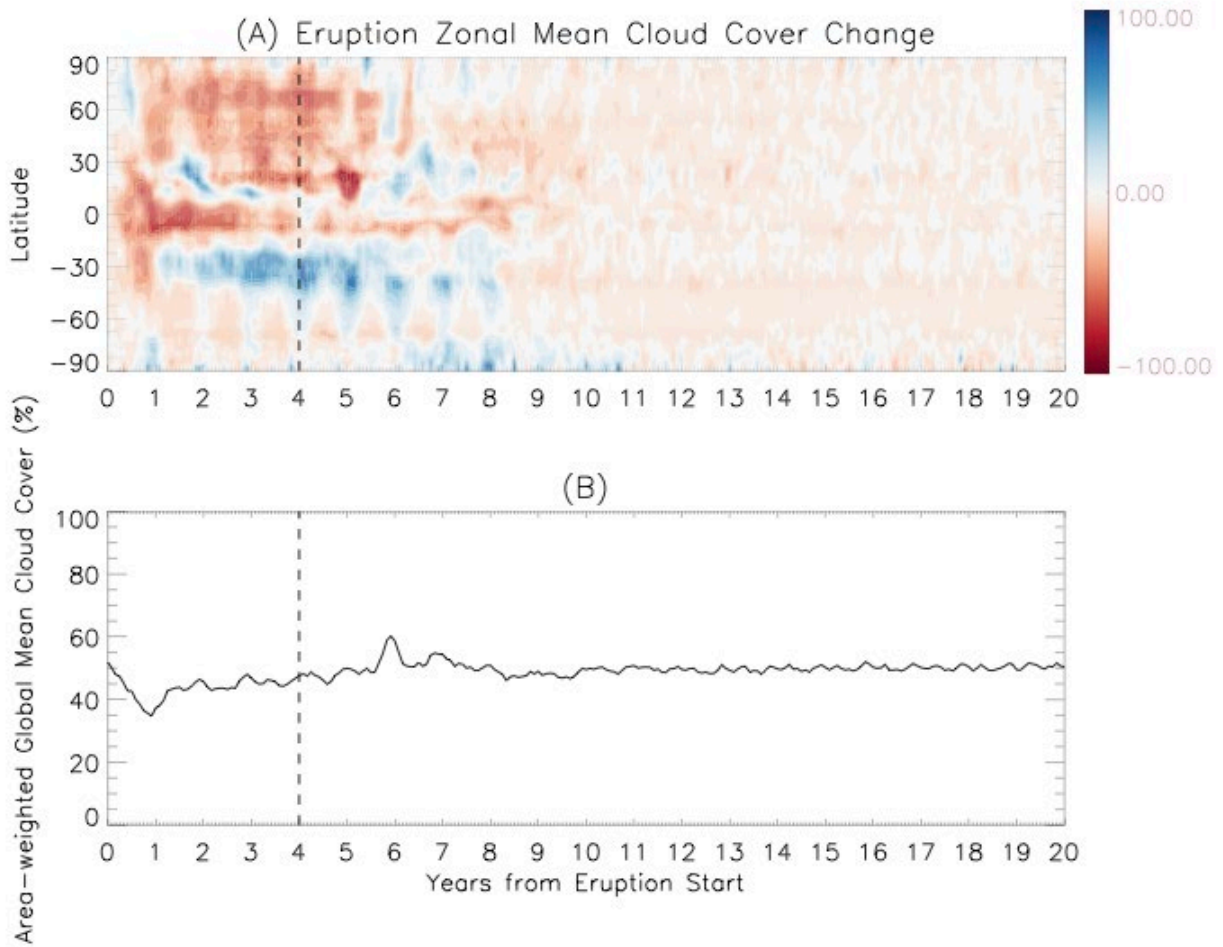


Fig. S5. Global change in cloud cover due to the eruption. (A) Zonal average change in cloud cover (%) relative to the baseline simulation as a function of time and (B) global area-weighted

cloud cover (%) in the eruption simulation. The vertical dashed line represents the end of the eruption.

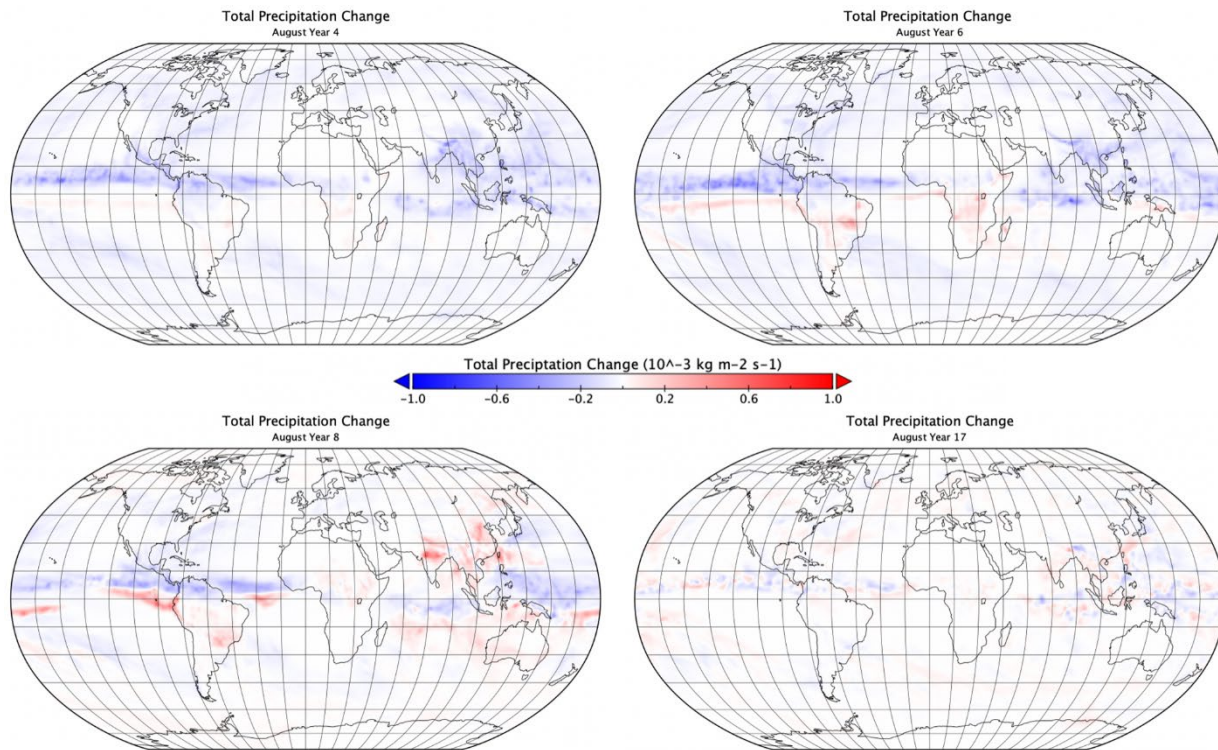


Fig. S6. Change in precipitation due to the eruption. Change (eruption-baseline) in total precipitation ($\text{kg m}^{-2} \text{ s}^{-1}$) for August in simulation years 4, 6, 8, and 17.

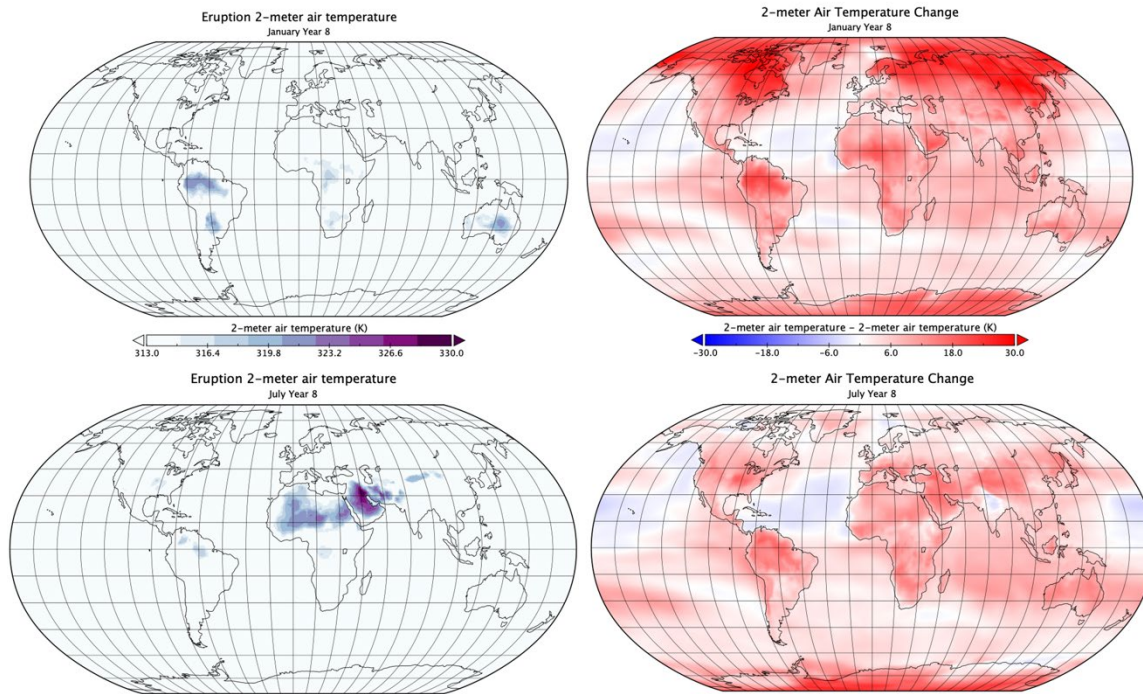


Fig. S7. Warming and extreme surface temperatures four years after the eruption ends. Monthly mean 2 m air temperatures in January and July of simulation Year 8 (left column) highlighting regions with mean monthly temperatures $\geq 40^{\circ}\text{C}$ ($\geq 313\text{ K}$). Change (eruption-baseline) in monthly mean 2 m air temperatures (K) in those same months (right column).